Journal of Quantitative Spectroscopy & Radiative Transfer 242 (2019) 106709

Contents lists available at ScienceDirect

Journal of Quantitative Spectroscopy & Radiative Transfer

journal homepage: www.elsevier.com/locate/jqsrt

Notes

The O_2 far-infrared absorption spectrum between 50 and 170 cm^{-1}

M. Toureille[a], S. Béguier[a], T.A. Odintsova[b], M.Yu. Tretyakov[b], O. Pirali[c,d], A. Campargue[a,*]

[a] Univ. Grenoble Alpes, CNRS, LIPhy, 38000 Grenoble, France
[b] Institute of Applied Physics, Russian Academy of Sciences, Nizhniy Novgorod, Russia
[c] SOLEIL Synchrotron, L'Orme des Merisiers, Saint-Aubin 91192, Gif-Sur-Yvette, France
[d] Institut des Sciences Moléculaires d'Orsay (ISMO), CNRS, Univ Paris Sud, Université Paris-Saclay, F-91405 Orsay, France

ARTICLE INFO

Article history:
Received 19 September 2019
Revised 16 October 2019
Accepted 17 October 2019
Available online 18 October 2019

Keywords:
Oxygen
O_2
Magnetic dipole
Far infrared
Synchrotron
SOLEIL
Line intensity

ABSTRACT

The oxygen absorption spectrum in the 50–170 cm^{-1} spectral range is studied at the AILES beam line of the SOLEIL synchrotron with a Fourier transform spectrometer equipped with a 151-m multipass gas cell. The spectrum recorded at room temperature (23.15 °C) with a pressure of 19.76 Torr is formed by weak pure rotational magnetic dipole transitions. Line parameters of 26 lines are derived and compared to literature values. In particular, measured line intensities confirm the 45 years-old previous values reported by Boreiko *et al.* (J. Quant. Spectrosc. Radiat. Transfer 32 (1984)109–117). The agreement with HITRAN intensities (within 1% level for the strongest lines) indicates that the 20% HITRAN error estimate was overly cautious: we show that the error is more likely within 2%.

1. Introduction

Being a homonuclear diatomic molecule, the $^{16}O_2$ oxygen molecule has no dipolar electric moment and thus no electric dipole-allowed rotational or vibrational bands. However, in the ground $X^3\sum_g^-$ state, two electron spins remain unpaired ($S=1$) which gives rise to a magnetic dipole moment. Weak magnetic dipolar transitions are thus observable in the ground electronic state as a fine-structure consisting of a *Q*-type branch near 60 GHz and a single line at about 119 GHz as well as the presently studied rotational *R*-type branch in the far infrared. The fine structure lines have been used by microwave radiometry for the atmosphere remote sensing for a long time [1]. The use of additional channels operating at the frequency of the rotational line near 425 GHz allows increasing accuracy of temperature and humidity profiles retrieval together with a better spatial resolution [2,3]. Corresponding instruments were developed [4] and considered for several missions such as the EU Geostationary Observatory for Microwave Atmospheric Sounding (GOMAS), the Geosynchronous Microwave (GEM) Sounder/Imager Observation System proposed by USA, the Chinese geostationary orbit meteorological Fengyun satellites, etc.

As a result of the spin-rotational interaction ($S=1$), each rotational level (N) of the ground $X^3\sum_g^-$ state splits into three components. It leads to a triplet multiplicity with total angular momentum $J=N$-1, N or $N+1$. Note that for the symmetric $^{16}O_2$ main isotopologue, only odd rotational levels exist in the ground state. The studied rotational magnetic dipole (M1) transitions follow thus the $\Delta N= +2$, $\Delta J= 0, +1$ selection rules leading to the observation of only two $\Delta N(N)\Delta J(J)$ branches: *SQ* and *SR*, respectively. Note that the *SQ(J)*, *SR(J)* and *SR(J-1)* lines have relative intensities of about 1, 0.3 and 0.2, respectively.

2. Experiment

The present recordings were performed during a measurement campaign at SOLEIL synchrotron devoted to the study of the H_2O–O_2 (and H_2O–N_2) foreign continuum of water vapor. The experimental set up is very similar to that previously used to study the far-infrared self-continuum of water vapor [5,6].

The spectrum was recorded at a pressure of 19.76 Torr measured with a Pfeiffer 100 mbar full range (stated uncertainty of 0.25% of the reading) using the standard mode of the synchrotron radiation and a multipass cell. The total absorption path length equals 151.75 ± 1.5 m corresponding to 60 passes between mirrors separated by 2.52 m and 0.5 m of space between windows. We recorded the spectrum using the FTIR Bruker IFS 125 spectrometer of the AILES beamline. The resolution (defined as 0.9/MOPD where MOPD is the maximum optical path difference) was set to 0.00102 cm^{-1} and no apodization of the interferogram was used

* Corresponding author.
E-mail address: alain.campargue@univ-grenoble-alpes.fr (A. Campargue).

https://doi.org/10.1016/j.jqsrt.2019.106709
0022-4073/

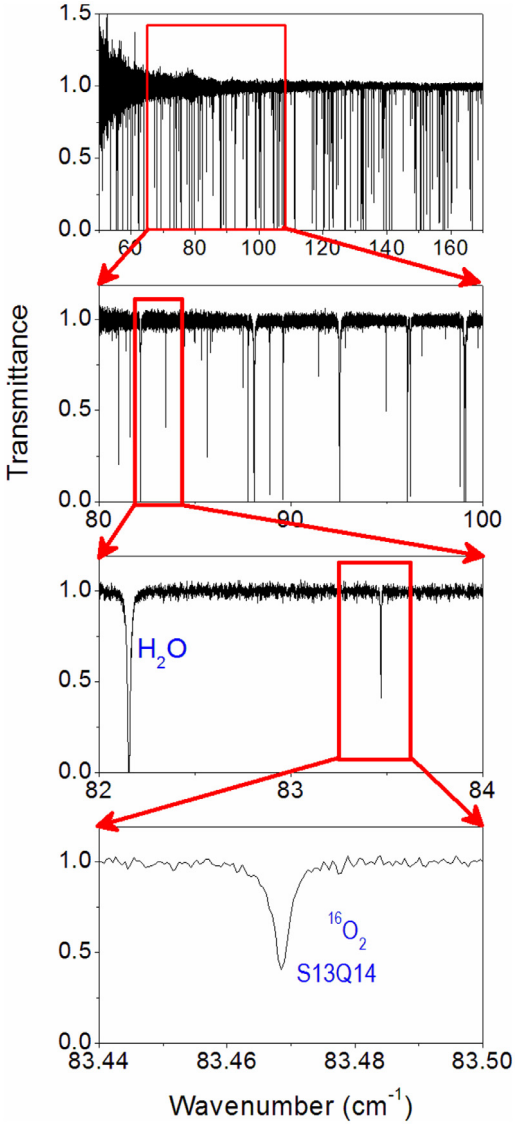

Fig. 1. Room temperature FTS absorption spectrum of oxygen ($P = 19.76$ Torr) recorded at SOLEIL synchrotron between 50 and 170 cm^{-1}. The spectrum is dominated by lines due to water present as an impurity with 40 ppm relative concentration. The last zoom shows the S13Q14 line of $^{16}O_2$ at 83.47 cm^{-1}.

(boxcar option of the Bruker software). A total of 290 interferograms were co-added. An overview of the transmittance spectrum is displayed on the upper panel of Fig. 1. Due to the very high intensity of the water lines in the region, the spectrum is dominated by water absorption present as an impurity (the relative water concentration was estimated to be 40 ppm, see below). Successive zooms are applied in Fig. 1 to show one of the strongest observed O_2 lines near 83.5 cm^{-1} (S13Q14).

3. Spectra analysis and results

The line parameters retrieval was performed using a homemade multiline fitting program in LabVIEW. In our pressure conditions, the pressure broadening (about 10^{-3} cm^{-1} HWHM at 19.76 Torr [7]) gives the dominant contribution to the line profile width. The contributions of the Doppler broadening (on the order of 10^{-4} cm^{-1} near 100 cm^{-1}) and of the apparatus function (about 3.5×10^{-4} cm^{-1} HWHM) are smaller. The FTS spectrum was fitted over a spectral interval around each O_2 line, using a Voigt line profile for the O_2 and the water interfering lines. The line position, line area and Lorentzian width were adjusted for each line. Fig. 2 shows the achieved line profile reproduction in the case of the isolated S13Q14 line. The residuals are at the noise level and correspond to a noise equivalent absorption on the order of 10^{-6} cm^{-1}. The relative concentration of water due to desorption from the cell walls was estimated to be about 40 ppm with a considerable $H_2{}^{18}O$ enrichment resulting from previous measurements of the self-continuum of water vapor with a sample highly enriched in ^{18}O [6].

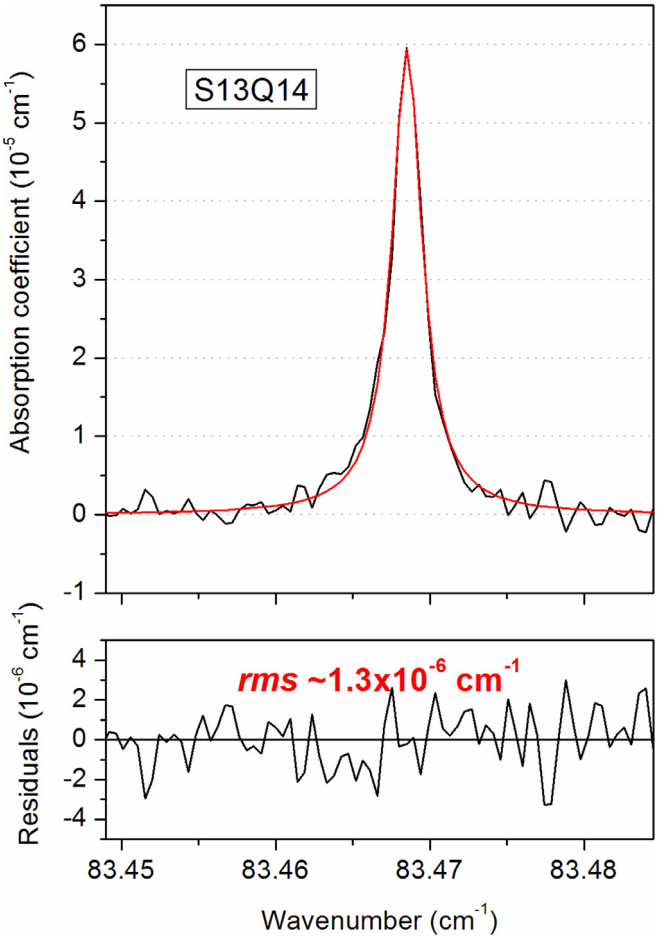

Fig. 2. Line profile fit of the S13Q14 line using a Voigt line shape and corresponding (obs.- calc.) residuals.

As a result, a list of twenty-six $^{16}O_2$ lines with intensity ranging between 7.8×10^{-27} and 5.0×10^{-25} cm/molecule was obtained (see Table 1). The list covers the S9R9-S25R26 and S9Q10-S27Q28 ranges of the SR and SQ branches (see Fig. 3).

4. Comparison to literature

The HITRAN positions of the considered lines were calculated by difference of the ground state energy levels obtained by Yu et al. [8] from an isotopically invariant Dunham fit of all the O_2 transitions available in the literature, in particular highly accurate microwave measurements. HITRAN line positions are provided with 10^{-6} and 10^{-5} cm^{-1} accuracy for positions below and above 90 cm^{-1}, respectively. Although agreeing with HITRAN values, our line positions determined with an accuracy no better than 5×10^{-5} cm^{-1} are insufficient to improve the accuracy of HITRAN positions.

To the best of our knowledge, the most recent laboratory measurement of the considered rotational lines was reported by Bor-

Table. 1
List of the rotational lines of $^{16}O_2$ measured by FTS between 50 and 170 cm^{-1}.

Transition	Position (cm^{-1})	Intensity at 296 K (cm/molecule)
S9R9	58.4153(4)	1.0(4)E-25
S9Q10	60.45547(7)	5.0(3)E-25
S9R10	62.3772(2)	1.5(5)E-25
S11R11	69.9077(2)	1.0(3)E-25
S11Q12	71.96900(7)	4.4(3)E-25
S11R12	73.8694(2)	1.4(2)E-25
S13R13	81.3866(3)	8(7)E-26
S13Q14	83.46851(5)	3.5(2)E-25
S13R14	85.3487(2)	8(3)E-26
S15R15	92.8514(3)	7(1)E-26
S15Q16	94.95289(6)	2.3(1)E-25
S15R16	96.8136(1)	7(1)E-26
S17R17	104.3007(8)	3(3)E-26
S17Q18	106.42091(7)	1.9(1)E-25
S17R18	108.2629(2)	5(2)E-26
S19R19	115.7317(4)	4(2)E-26
S19Q20	117.8708(1)	1.1(1)E-25
S19R20	119.6943(1)	2.1(9)E-26
S21R21	127.1435(3)	1.2(5)E-26
S21Q22	129.3011(1)	7.0(7)E-26
S21R22	131.1068(2)	1.1(5)E-26
S23R23	138.5347(3)	8(4)E-27
S23R24	142.4977(3)	9(5)E-27
S25Q26	152.0961(6)	1.0(7)E-26
S25R26	153.8655(7)	1.1(6)E-26
S27Q28	163.457(1)	1.0(7)E-26

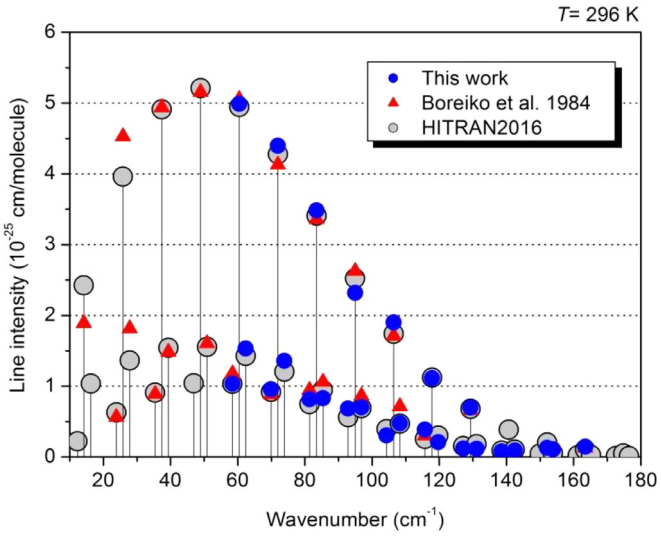

Fig. 3. Overview of the rotational magnetic dipole transitions of $^{16}O_2$ between 10 and 180 cm^{-1}: line lists provided by HITRAN2016 [7] (open grey circles), measured by Boreiko *et al.* [9] (red triangles) and measured in the present work (blue circles).

eiko *et al.* in 1984 [9]. These authors used a high pressure Hg arc source, a multipass White cell providing a 45.1 mpath length and performed FTS recordings with a spectral resolution of 0.07 cm^{-1}, for a series of pressures ranging between 52 and 672 Torr. Their measurements of 23 lines extend down to 14 cm^{-1} but only one line was reported above 130 cm^{-1} (see Fig. 3). Particular care was devoted to the intensities determination from the proportionality factor between the equivalent widths of the lines and the recording pressures [9]. As a result, the (statistical) error bars attached to the measured intensities are small, on the order of 1%.

Although showing a dispersion larger than 1%, the intensity comparison between HITRAN values and the values reported by Boreiko *et al.* is on average very good (see Fig. 4, middle panel). The HITRAN intensity values were calculated by Mackie using a global intensity model [7]. We do not know if the measurements of

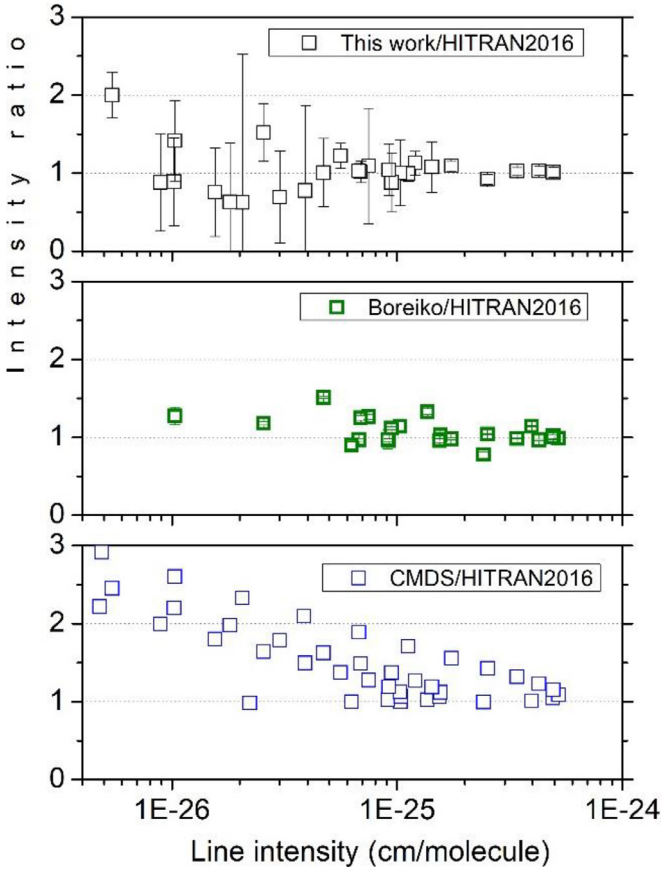

Fig. 4. Comparison to HITRAN values of the intensities the $^{16}O_2$ lines between 10 and 180 cm^{-1} from different sources: present measurements (open squares), measurements by Boreiko *et al.* [9] (open green squares), provided by CDMS [12–14] (blue open squares).

Ref. [9] were used to scale the calculated values but the agreement is excellent.

Our intensity values derived from a single FTS spectrum recorded with a ten times better spectral resolution and a smaller pressure fully confirm the intensity results by Boreiko *et al.* In spite of larger statistical error bars, the overall agreement with HITRAN for the lines with intensity larger than 10^{-25} cm/molecule is similar or even better than that obtained with the values of Boreiko *et al.* (see Fig. 4 upper panel). HITRAN intensity values are provided with 20% error bar. The overall agreement indicates that HITRAN error bars are largely overestimated and could be reduced to 2% at least for the strongest lines. Note that a similar situation was found for the first rotational triplet. Measurements of the S1R1 and S1Q2 lines at 368 and 425 GHz, respectively, in pure oxygen and in air by resonator technique at room temperature and atmospheric pressure were performed with a statistical uncertainty of about 5% but the measured values agree with HITRAN within 1–3% [10].

The GEISA database [11], the Cologne Database for Molecular Spectroscopy (CDMS) [12–14] and the catalogue elaborated at Jet Propulsion Laboratory (JPL) [15] provide alternative line lists for the considered O_2 transitions. The GEISA and JPL intensities coincide with HITRAN values. Fig. 4 includes a comparison of the HITRAN values to the CDMS intensities. While the lowest J transitions have CDMS intensities coinciding to HITRAN values, the highest J transitions ($J \sim 30$) have an intensity overestimated by a factor of more than two. The intensity adjustment applied to JPL intensities in March 2014 is intended to be applied to the CDMS catalogue in the near future.

Declaration of Competing Interest

None.

Acknowledgements

This work became possible due to the Project No 20180347 supported by SOLEIL Synchrotron Team. TAO and MYT acknowledge the support from Presidium RAS Program No. 5.

References

[1] Woodhouse IH. Introduction to microwave remote sensing. Boca Raton: Taylor & Francis, CRC Press; 2006.
[2] Zhao HB, Zheng C, Zhang YF, Liang B, Ou NM, Miao JG. Information content analysis for the millimeter and sub-millimeter wave atmospheric sounding data from geostationary orbit. Prog Electromagn Res M 2014;35:183–91.
[3] Wang R, Wang Y, Yan W, Lu W, Ma S, Zhao X, Gu C. Channel selection, data simulation, and parameter inversion of ground-based hyperspectral microwave radiometer. Math Probl Eng. 2019; Art. ID: 4846378. doi:10.1155/2019/4846378.
[4] Leslie RV, Staelin DH. NPOESS aircraft sounder testbed-microwave: observations of clouds and precipitation at 54, 118, 183, and 425 GHz. IEEE Trans Geosci Remote Sens 2004;42(10):2240–7.
[5] Odintsova TA, Tretyakov MY, Pirali O, Roy P. Water vapor continuum in the range of rotational spectrum of H_2O molecule: new experimental data and their comparative analysis. J Quant Spectrosc Radiat Transf 2017;187:116–23. doi:10.1016/j.jqsrt.2016.09.009.
[6] Odintsova TA, Tretyakov MY, Zibarova AO, Pirali O, Roy P, Campargue A. Far-infrared self-continuum absorption of $H_2{}^{16}O$ and $H_2{}^{18}O$ (15–500 cm^{-1}). J Quant Spectrosc Radiat Transf 2019;227:190–200. doi:10.1016/j.jqsrt.2019.02.012.
[7] Gordon IE, Rothman LS, Hill C, Kochanov RV, Tan Y, Bernath PF, Birk M, Boudon V, Campargue A, Chance KV, Drouin BJ, Flaud J-M, Gamache RR, Hodges JT, Jacquemart D, Perevalov VI, Perrin A, Shine KP, Smith MAH, Tennyson J, Toon GC, Tran H, TyuterevVIG, Barbe A, Császár AG, Devi VM, Furtenbacher T, Harrison JJ, Hartmann J-M, Jolly A, Johnson TJ, Karman T, Kleiner I, Kyuberis AA, Loos J, Lyulin OM, Massie ST, Mikhailenko SN, Moazzen-Ahmadi N, Müller HSP, Naumenko OV, Nikitin AV, Polyansky OL, Rey M, Rotger M, Sharpe SW, Sung K, Starikova E, Tashkun SA, Vander Auwera J, Wagner G, Wilzewski J, Wcisło P, Yu S, Zak EJ. The HITRAN2016 molecular spectroscopic database. J Quant Spectrosc Radiat Transf 2017;203:3–69. doi:10.1016/j.jqsrt.2017.06.038.
[8] Yu S, Drouin BJ, Miller CE. High resolution spectral analysis of oxygen. IV. Energy levels, partition sums, band constants, RKR potentials, Franck–Condon factors involving the $X^3\Sigma^-_g$, $a^1\Delta_g$ and $b^1\Sigma^+_g$ states. J Chem Phys 2014;141:174302. doi:10.1063/1.4900510.
[9] Boreiko RT, Smithson TL, Clark TA, Wieser H. Line strengths and positions of the submillimeter magnetic dipole transitions of O_2. J Quant Spectrosc Radiat Transf 1984;32:109–17.
[10] Tretyakov MYu, Koshelev MA, Vilkov IN, Parshin VV, Serov EA. Resonator spectroscopy of the atmosphere in the 350–500 GHz range. J Quant Spectrosc Rad Transf 2013;114:109–21.
[11] Jacquinet-Husson N, Armante R, Scott NA, Chedin A, Crepeau L, Boutammine C, et al. The 2015 edition of the GEISA spectroscopic database. J Mol Spectrosc 2016;327:31–72. doi:10.1016/j.jms.2016.06.007.
[12] Endres CP, Schlemmer S, Schilke P, Stutzki J, Müller HSP. The cologne database for molecular spectroscopy, CDMS, in the virtual atomic and molecular data centre. VAMDC J. Mol. Spectrosc 2016;327:95–104.
[13] Müller HSP, Thorwirth S, Roth DA, Winnewisser G. The cologne database for molecular spectroscopy; astron. Astrophys 2001;370:L49–52.
[14] https://cdms.astro.uni-koeln.de/.
[15] https://spec.jpl.nasa.gov/ftp/pub/catalog/catform.html.